

Structural analysis of high-rise buildings under horizontal loads: A study on the Intesa Sanpaolo Tower in Turin



Alberto Carpinteri, Giuseppe Lacidogna*, Sandro Cammarano

Department of Structural, Geotechnical and Building Engineering, Politecnico di Torino, C.so Duca degli Abruzzi 24, Torino, Italy

ARTICLE INFO

Article history:

Received 18 December 2012

Revised 31 May 2013

Accepted 5 July 2013

Keywords:

Structural behaviour

Analytical method

Tall buildings

Lateral load distribution

Thin-walled cross section

Braced frames

Vlasov's theory

ABSTRACT

In the last decades, the expansion of high-rise buildings has reached even those countries in which the past architectural conceptions and the municipal regulations have hampered their construction. Suffice it to say that in Turin (Italy), in the last few years, two tall buildings have been designed, both with an height comparable to the Mole Antonelliana, which has so far been the major landmark building of the city. The design of these structures is very complex. Indeed, from the structural viewpoint, the horizontal actions caused by wind and earthquakes represent a key issue for the designers. Therefore, the choice of an appropriate model able to thoroughly identify the foremost parameters governing the response of the structure is all along crucial. For this purpose, in this paper the three-dimensional formulation of Carpinteri et al. (2010) [32], which evaluates the displacements and the lateral load distribution of external actions in tall buildings having any combination of bracings, is reviewed. The present work evaluates the effectiveness of the method by means of a numerical example regarding the 39-storey (166 m) Intesa Sanpaolo Tower, designed by Renzo Piano. The results are compared, in terms of displacements and rotations, with those shown in the final project of the building. Finally curves concerning the main internal actions of a single bracing are presented.

© 2013 Elsevier Ltd. All rights reserved.

1. Introduction

A quick expansion of high-rise buildings took place in the last century. Initially most of them were arranged where the economic capability was large and the technological progress in constructions was on the cutting edge. Now their development is spreading throughout the world, even in countries which are experiencing a fast industrial growth. Among them, we could include China, Korea, India, Taiwan and Malaysia. This type of structure is also gaining ground in those countries, in which the past architectural conceptions and the municipal regulations have hampered their construction. Some European countries represent a glaring proof of this new trend. In Turin (Italy), for example, in the last few years, two tall buildings have been designed, being already under construction the 39-storey (166 m) Intesa Sanpaolo Tower by Renzo Piano (Fig. 1).

From the structural viewpoint, high-rise structures represent a demanding problem which requires adequate structural solutions in terms of stability and rigidity. Indeed, while in the design of low-rise buildings the influence of dead and live loads is the leading factor, increasing height, the attention of the structural engineers

focuses on the need to control the horizontal displacements. The higher the building, the more sensitive it becomes to horizontal actions, coming from wind and earthquakes. Without specific stiffening members, the dimensions of the columns increase to such an extent that they are no longer reasonable from an architectural point of view. For this reason, the traditional solutions providing vertical bearing capacity tend to be associated with or, in some cases, replaced by innovative structural systems, which evolved from rigid frame, tube, core-outrigger to diagrid structures.

Behind the latter architectural trends, the idea that the building could be described as a single element projecting out from the ground has emerged, giving the opportunity to reduce the structure to a simpler rigid member as a single cantilever or a system of cantilevers.

This highlights that the key issue in structural design is the choice of an appropriate model which is able to reproduce with a good approximation the actual behaviour of the building, as well as to allow an accurate understanding of the force flow within the stiffeners.

By now, in the last decades, Finite Elements (FE) models have achieved a wide agreement in the engineering community since they represent a powerful tool for the analysis of very complex structures. With the help of fast computers, they allow to obtain comprehensive results on the global behaviour of the building and, at the same time, to deepen any level of detail, in order to

* Corresponding author. Tel.: +39 0110904871.

E-mail address: giuseppe.lacidogna@polito.it (G. Lacidogna).

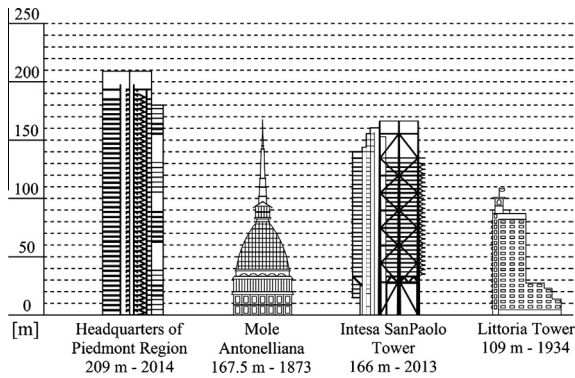


Fig. 1. Comparison between tall buildings in Turin, Italy.

develop a high degree of accuracy. This allows the structural designer to take into account every possible solution to satisfy the architectural requirements of the patrons and, somehow, makes him believe to have achieved an exhaustive knowledge of the problem. It should be considered partially true. On one hand, the accuracy of the method ensures a numerical solution, on the other, it could divert attention from an analysis aimed to detect the structural parameters governing the response of the structure.

In addition, at early stages of the design process, the choice of these methods may not be appropriate. The procedure of data preparation and modelling is often lengthy and time-consuming, especially during the phase of evolution of the concept in which several structural configurations may be proposed in order to evaluate the resistant contributions coming from different stiffening solutions. At the same time, the huge amount of input and output data could easily cause misunderstandings which impede a clear explanation of the structural mechanism and do not allow the designers to define unequivocally the distribution of the external forces amongst stiffening elements.

As remarked by Howson [1], this does not intend to deny the usefulness and the potentiality of FE models, but rather sensitise the design community in order to consider the issue in its entirety without reducing it to a mere numerical estimate.

From this point of view, simplified procedures relying on carefully chosen approximations may become an effective tool for the structural planning. In fact, since a narrow number of variables is taken into account, the phases of data preparation and modelling are definitely faster and clearer. In particular, the analysis can evolve more transparently, thus making the process less liable to unexpected errors. Moreover, as regards the accuracy, the level achieved by the analytical methods, even though low compared to that in FE simulations, is enough to obtain a preliminary estimate of the resistant mechanism of the bearing elements. And lastly, through the definition of simplified hypotheses, it is possible to identify the key structural parameters, which are at the base of the conceptual design. As an example, one could define the interaction among the horizontal stiffeners in order to have a comprehensive picture of the structural behaviour.

It is clear that the effectiveness of these analytical methods depends on the initial assumptions, which require a careful assessment by the designers. As a matter of fact, just this allows the engineer to play a leading role in a very tricky phase of the construction process. Therefore, both approaches may be considered reciprocally complementary instruments and so can lend support to the engineer's judgment on two different levels. On one hand, in the early stages, approximate methods could evaluate the basic characteristics of the project; on the other, as regards the final stages, FE models could conduct a detailed analysis by means of a more thorough computation.

The earliest analytical models, which attempted to assess the lateral resistant mechanism of high-rise buildings, focused on the plane behaviour of the stiffeners and their mutual interaction. This means that only one degree of freedom per storey is considered, as well as the torsional analysis is separated from the flexural one. That is the case of the shear wall versus frame interaction, developed in the 1960s and 1970s, among all, by Khan and Sbarounis [2], Coull and Irwin [3], Heidebrecht and Stafford Smith [4], Rutenberg and Heidebrecht [5] and Mortelmans et al. [6].

Another model, concerning the analysis of coupled shear wall structures, is based on the continuum medium technique proposed in the pioneering papers by Rosman [7] and Beck et al. [8,9], in which the whole structure is idealized as a single shear-flexural cantilever. The principle of the method is to replace the effect of individual beams or slabs, which interconnect the walls at each floor, by continuously distributed shear forces, that concur to stiffen the structural behaviour. This method was later extended in order to include other structural typologies as shown by Stafford Smith and Coull [10], Hoenderkamp and Snijder [11] and Lee et al. [12], or consider further effects such as the axial deformation in frames, as indicated by Swaddiwudhipong et al. [13]. In line with the continuum medium technique, other works underline the high stiffening contribution due to the presence of connecting beams or slabs. Among all, the papers by Heidebrecht and Swift [14], Tso and Biswas [15] and Capuani et al. [16] are noteworthy.

According to the development of tall building typologies, we could cite other models concerning framed wall structures, as in the papers by Stamato and Mancini [17], Gluck and Krauss [18], as well as framed-tube structures, as in the papers by Khan [19], Coull and Bose [20].

A different research direction, derived from aerospace engineering, is based on the subdivision of the structure into substructures; it is somehow in between the simplified models and the FE approach, since the substructures are used to formulate super-elements, either by condensation or by analytical procedures with exact solutions. Among others, we could cite the papers by Leung [21], Leung and Wong [22], Wong and Lau [23], as well as the so-called finite storey method (FSM) by Pekau et al. [24,25]. More recent works include, among others, the approaches presented by Kim and Lee [26] and Steebergen and Blaauwendraad [27].

The main drawback of these simplified models is the lack of generality. Since they are often reduced to consider specific resistant schemes, they can hardly be used to analyse, at the same time, different underlying structural typologies. Moreover, being faced with more complex architectural shapes, a plane model is liable to become unsuitable to describe with a good approximation the behaviour of innovative buildings.

With the aim to define a general method able to take into account the main stiffening elements, usually adopted in high-rise buildings, as well as their arrangement within an unconventional structural scheme, in this paper we propose a three-dimensional formulation based on the work by Carpinteri and Carpinteri [28]. The latter has been extended to encompass any combination of bracings, including bracings with open thin-walled cross-sections, which are analysed in the framework of Timoshenko-Vlasov's theory [29,30] of sectorial areas and according to the approach by Capurso [31], as recently proposed by Carpinteri et al. [32,33].

In order to evaluate the effectiveness and the flexibility of the model, a numerical example regarding the 39-storey (166 m) Intesa Sanpaolo Tower, designed by Renzo Piano, is carried out, in which all the resistant contributions coming from different stiffening elements are highlighted. A comparison, in terms of displacements, with the values reported in the final project by the designers involved in the construction, assesses the accuracy of the results.

2. Analytical formulation

This section presents the general formulation regarding the problem of the external lateral load distribution between the bracings of a three-dimensional civil structure, originally proposed by Carpinteri and Carpinteri [28].

The model is supported by some simplifying assumptions:

- (1) The material of the resistant elements is homogeneous, isotropic and obeys Hooke's law.
- (2) The floor slabs are rigid in their plane, while the out-of-plane rigidity is negligible.
- (3) The load is defined by conservative forces.
- (4) The axial deformation of the bracings is neglected.

The horizontal resistant skeleton of the building is composed by M bracings connected each other through rigid floors. Only three degrees of freedom (DOF) are considered for each storey: the two translations, ξ and η in the X and Y directions of the global coordinate system origin (Fig. 2), and the floor rotation, ϑ . Being N the number of the storeys, the total number of DOFs is $3N$. Similarly the external load is represented by a $3N$ -vector \mathbf{f} , whose elements are described by three forces for each floor and, more exactly, two shear forces, p_x and p_y , and the torsional moment m_z . If \mathbf{p} is the $2N$ -vector describing the shear forces and \mathbf{m} the N -vector for the torsional moments, the external loading vector may be represented as

$$\mathbf{f} = \begin{Bmatrix} \mathbf{p} \\ \mathbf{m} \end{Bmatrix}. \quad (1)$$

On the other hand, the vector \mathbf{f}_i represents the internal loading vector transmitted to the i th element and related to the global coordinate system XY (Fig. 3), as well as \mathbf{f}_i^* is the internal loading vector related to the local coordinate system $X_i^*Y_i^*$ (the origin of this system is the shear centre and the axes are the principal ones as regards the section of the bracing). The latter may be connected with the former by means of the matrix \mathbf{A}_i , as follows:

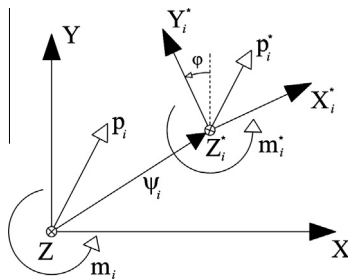


Fig. 2. Global and local coordinate systems. The Z axis completes the right-handed global system XYZ and Z_i^* completes the right-handed local system $X_i^*Y_i^*Z_i^*$.

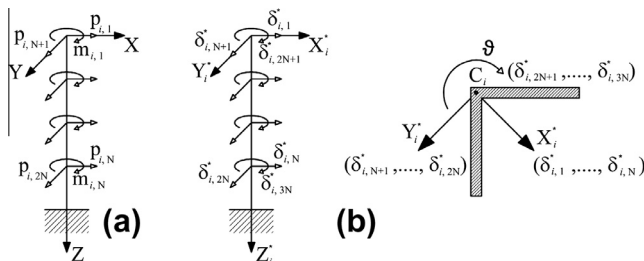


Fig. 3. Internal loading \mathbf{f}_i transmitted to the i th bracing in the global coordinate system (a). Degrees of freedom of the i th bracing in the local coordinate system $X_i^*Y_i^*Z_i^*$, axonometry and top view (b).

$$\mathbf{f}_i^* = \mathbf{A}_i \mathbf{f}_i, \quad (2)$$

where

$$\mathbf{A}_i = \begin{bmatrix} \mathbf{N}_i & \mathbf{0} \\ -\mathbf{C}_i^T & \mathbf{I} \end{bmatrix}. \quad (3)$$

The $2N \times 2N$ -matrix \mathbf{N}_i is the orthogonal rotation matrix from the system XY to the system $X_i^*Y_i^*$ through the angle φ between the Y axis and the Y_i^* axis (Fig. 2); \mathbf{I} is the identity matrix, $\mathbf{0}$ the null matrix and the $N \times 2N$ -matrix \mathbf{C}_i^T is defined as

$$\mathbf{C}_i^T = [-\mathbf{y}_i \ \mathbf{x}_i], \quad (4)$$

where each element is a diagonal $N \times N$ -matrix and (x_i, y_i) are the coordinates of the origin of the local system $X_i^*Y_i^*$ in the global one XY .

In the same way, the displacements δ_i related to the i th bracing in the global coordinate system are connected with the displacements δ_i^* , which refer to the local system, through the matrix \mathbf{B}_i .

$$\delta_i^* = \mathbf{B}_i \delta_i, \quad (5)$$

where

$$\mathbf{B}_i = \begin{bmatrix} \mathbf{N}_i & \mathbf{0} \\ \mathbf{0} & \mathbf{I} \end{bmatrix}. \quad (6)$$

If we take into account the structural behaviour of the i th bracing, related to its principal coordinate system, we get the following relation

$$\mathbf{f}_i^* = \mathbf{K}_i^* \delta_i^*, \quad (7)$$

\mathbf{K}_i^* being the corresponding condensed stiffness matrix.

Substituting Eqs. (2) and (5) into Eq. (7) and pre-multiplying both the members by the inverse of \mathbf{A}_i , a relation between \mathbf{f}_i and δ_i is obtained:

$$\mathbf{f}_i = (\mathbf{A}_i^{-1} \mathbf{K}_i^* \mathbf{B}_i) \delta_i. \quad (8)$$

Through Eq. (8) the stiffness matrix of the i th bracing in the global coordinate system XY is highlighted:

$$\mathbf{K}_i = \mathbf{A}_i^{-1} \mathbf{K}_i^* \mathbf{B}_i. \quad (9)$$

Since the degrees of freedom of the problem are expressed in terms of floor displacements, the $3N$ -vector δ_i may be reduced to the displacement $3N$ -vector δ of the storeys by the relation

$$\delta_i = \mathbf{T}_i \delta, \quad (10)$$

where the $3N \times 3N$ -matrix \mathbf{T}_i is the transformation matrix, defined by the matrix \mathbf{C}_i of Eq. (4):

$$\mathbf{T}_i = \begin{bmatrix} \mathbf{I} & \mathbf{C}_i \\ \mathbf{0} & \mathbf{I} \end{bmatrix}. \quad (11)$$

Eq. (8) can be rewritten:

$$\mathbf{f}_i = \mathbf{K}_i \mathbf{T}_i \delta = \bar{\mathbf{K}}_i \delta, \quad (12)$$

where $\bar{\mathbf{K}}_i = \mathbf{K}_i \mathbf{T}_i$ is the stiffness matrix of the i th element with respect to the floor displacements.

For the global equilibrium we have:

$$\mathbf{f} = \sum_{i=1}^M \mathbf{f}_i = \sum_{i=1}^M \bar{\mathbf{K}}_i \delta. \quad (13)$$

So

$$\mathbf{f} = \bar{\mathbf{K}} \delta, \quad (14)$$

where $\bar{\mathbf{K}}$ is the global stiffness matrix of the system.

Recalling Eqs. (12) and (14), we get:

$$\delta = \bar{\mathbf{K}}_i^{-1} \mathbf{f}_i = \bar{\mathbf{K}}^{-1} \mathbf{f}, \quad (15)$$

and then:

$$f_i = \bar{K}_i \bar{K}^{-1} f. \tag{16}$$

Eq. (16) solves the problem of the external loading distribution between the resistant elements used to horizontally stiffen a building. As the case of in-parallel bracings in a plane problem, even in this case the loading distribution matrix is given by the “ratio” of the partial stiffness matrix, related to the *i*th element, to the total stiffness matrix of the system.

Such a formulation proves to be general and may be adopted with any kind of structural elements, having closed or open sections, constant or variable along the height.

As regard the implementation of the method, only basic information are needed: the geometry, the material and the location of the different horizontal bracings as well as the intensity of the

loads. If these information are known, the procedure of data preparation is really brief and, for very complex structures, it can be even developed in half a day.

The effectiveness of the formulation is confirmed by the next section in which a numerical example regarding the 39-storey Intesa Sanpaolo Tower (Turin, Italy) is shown.

3. Numerical example

This section focuses on the development of a numerical example regarding the lateral load distribution of external actions between different types of bracings commonly used to stiffen high-rise buildings. This is the case of frames, braced frames, thin-walled open or closed section shear walls. The investigated structure is the Intesa Sanpaolo Tower, designed by Renzo Piano and still under construction in Turin (Italy). It is composed of 39 storeys, having not a constant height. The total height of the building is *H* = 166 m. The horizontal resistant skeleton is symmetric from South to North, while, in the orthogonal direction, when the structure is subjected to horizontal loads, such an arrangement gives rise to coupling between flexural and torsional behaviour.

In the south facing portion, the building is supported by steel columns and beams constituting a system of frames and braced frames in both principal directions; on the opposite side, the stiffening contribution is provided by a system of concrete shear walls, most of which having a thin-walled open section.

In Fig. 4 the foremost components of the resistant skeleton of the building as well as the global coordinate system *XY*, to which the loading and displacement vectors are referred, are highlighted.

Each type of bracing is modelled by considering its local coordinate system, in order to obtain the respective stiffness matrix K_i^* , which may be used in the general formulation proposed in Section 1, in particular it may be directly inserted into Eq. (7).

As regards the construction materials, Young’s modulus for concrete is $E_c = 4.0 \times 10^4$ MPa, whereas for steel $E_s = 21.0 \times 10^4$ MPa; the Poisson ratio is $\nu_c = 0.18$ and $\nu_s = 0.3$, respectively. The influence of creep and shrinkage are not taken into account in the analysis. The geometric dimensions of the shear walls are shown

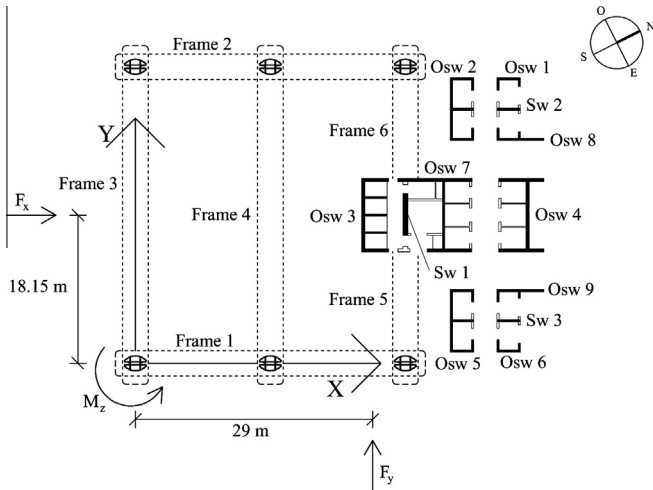


Fig. 4. Planimetric layout of the Intesa Sanpaolo Tower showing the main horizontal resistant members: shear walls (Sw), thin-walled open section shear walls (Osw) and frames.

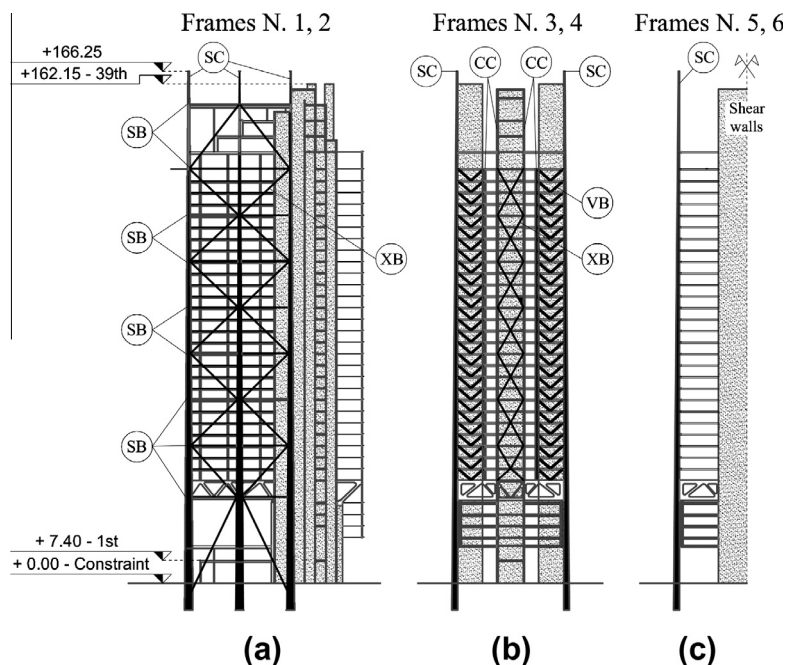


Fig. 5. Structural schemes of the frames in which the main elements are highlighted: tapered steel columns (SC), concrete columns (CC), steel beams (SB), V-bracings (VB) and X-bracings (XB).

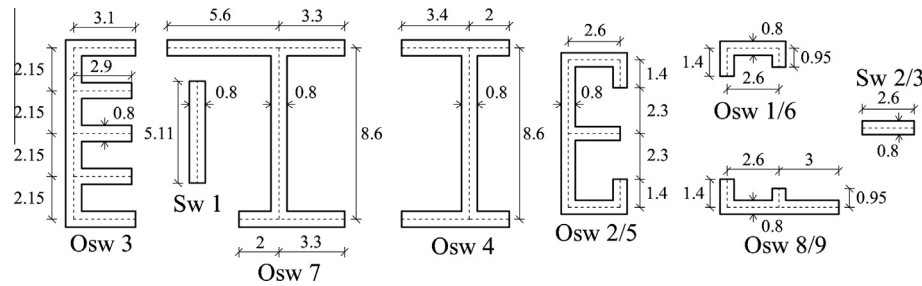


Fig. 6. Geometric dimensions of the shear walls, in metres.

Table 1
Cross-section properties of the shear walls.

Shear wall No.	1	2	3
Area (m ²)	4.09	2.08	2.08
Second moment ^a J_{xx} (m ⁴)	8.90	0.11	0.11
Second moment ^a J_{yy} (m ⁴)	0.22	1.17	1.17
Torsional rigidity à la de Saint Venant (m ⁴)	0.87	0.44	0.44
Global coordinate x_c of the shear centre (m)	33.02	45.63	45.63
Global coordinate y_c of the shear centre (m)	18.22	31.10	5.20
Angle ^b φ (°)	0.00	0.00	0.00

^a Related to the centroidal principal axes of the section.

^b Between the centroidal principal axes and the XY axes.

in Fig. 6; the corresponding cross-section properties, reported in Tables 1 and 2, are calculated taking into account the mid line of the sections.

The geometric dimensions and the resistant properties of the elements constituting the frames are reported in Table 3. As regards frames 1 and 2, we consider the scheme (a) of Fig. 5, whereas

schemes (b) and (c) describe the others. The main vertical elements are the steel columns, tapered along the height. In the scheme (a) the connections between diagonal bracings and columns are performed by means of steel beams in place of concrete beams, which are used at other floors. In the scheme (b), other four concrete columns are present which allow the connection of V- and X-bracings.

It should be noted the absence of resistant beams in the bottom and top part of the frames (Fig. 5). This is due to the presence of a winter garden at the top and an auditorium at the bottom. For these reasons, huge truss beams have been designed in order to transfer vertical loads coming from the upper floors to the outer steel columns. From the structural viewpoint, this choice represents a discontinuity for the stiffness of these elements.

The building foundation is an huge cubic box supported by a rigid slab of 4 m in height and constituted by five underground floors, each of 3600 m². In this way, by means of this configuration, it is possible to consider the building as if it is directly constrained at the ground floor.

Concerning the loads, in this paper only wind actions are considered, as well as reported in the examined project of the building.

Table 2
Cross-section properties of the thin-walled open section shear walls.

Open section shear wall No.	1	2	3	4	5	6	7	8	9
Area (m ²)	3.96	14.4	18.8	15.52	14.4	3.96	18.24	6.36	6.36
Second moment ^a J_{xx} (m ⁴)	0.58	104.49	155.56	202.16	104.49	0.58	254.07	0.60	0.60
Second moment ^a J_{yy} (m ⁴)	4.34	15.72	18.58	22.87	15.72	4.34	56.48	18.97	18.97
Warping moment ^c $J_{\omega\omega}$ (m ⁶)	0.56	208.74	160.95	404.62	208.74	0.56	650.43	1.06	1.06
Torsional rigidity à la de Saint Venant (m ⁴)	0.84	3.07	4.01	3.31	3.07	0.84	3.89	1.36	1.36
Global coordinate x_c of the shear centre (m)	45.10	37.19	26.76	48.49	37.19	45.10	37.45	45.08	45.08
Global coordinate y_c of the shear centre (m)	35.18	31.10	18.15	18.15	5.20	1.12	20.97	27.32	8.98
Angle ^b φ (°)	6.38	0.00	0.00	0.00	0.00	-6.38	13.02	-5.25	5.25

^a Related to the centroidal principal axes of the section.

^b Between the centroidal principal axes and the XY axes.

^c Related to the shear centre of the section and to the principal diagram of the warping function.

Table 3
Structural elements constituting the frames.

Element	Section shape	Geometric property	Frame No.					
			1	2	3	4	5	6
Tapered mega-column	Rectangular 1.9 × 1.28 m (at the base) 0.35 × 0.23 m (on the top)	Second moment J_{xx} (m ⁴) (min)	8.2E-04	8.2E-04	8.2E-04	8.2E-04	8.2E-04	8.2E-04
		Second moment J_{xx} (m ⁴) (max)	7.3E-01	7.3E-01	7.3E-01	7.3E-01	7.3E-01	7.3E-01
		Second moment J_{yy} (m ⁴) (min)	3.5E-04	3.5E-04	3.5E-04	3.5E-04	3.5E-04	3.5E-04
		Second moment J_{yy} (m ⁴) (max)	3.3E-01	3.3E-01	3.3E-01	3.3E-01	3.3E-01	3.3E-01
Concrete Column	Square 0.4 × 0.4 m	Second moment J_{xx} (m ⁴)	-	-	2.1E-03	2.1E-03	-	-
Concrete beam	Square 0.3 × 0.3 m	Second moment J (m ⁴)	6.8E-04	6.8E-04	2.1E-03	2.1E-03	2.1E-03	2.1E-03
Steel beam	Circular hollow ϕ 350 (t 40)	Second moment J (m ⁴)	1.1E-02	1.1E-02	-	-	-	-
X-bracing	ϕ 140/160	Area (m ²)	3.1E-02	3.1E-02	4.0E-02	-	-	-
V-bracing	UPN 180 (2)	Area (m ²)	-	-	5.6E-03	-	-	-
Global coordinate x (m)			16.50	16.50	0.00	16.50	33.00	33.00
Global coordinate y (m)			0.00	36.30	18.15	18.15	0.00	36.30
Angle φ (°)			0.00	0.00	90.00	90.00	90.00	90.00

Due to the hypothesis of infinite rigidity of the floors in their plane, the wind action may be reduced to a system of concentrated horizontal loads, applied to the barycentre of the pressure distribution, for both principal directions. The intensity of the action is computed according to the formulas indicated by the Italian Technical Regulations [34], which propose the same methods contained in the Eurocode 1 [35]. Thus, the wind action may be considered as a static load, acting along the principal axes of the structure.

The evaluation of the wind action, proposed by the Eurocode 1, depends on the size, shape and dynamic properties of the building and involves the computation of some terms. First of all, the reference velocity v_b of the wind, which is a function of the region and altitude of the location. For this specific case (wind zone 1 and altitude equal to 240 m), it is equal to 25 m/s. Since the expected nominal life of the building is 100 years, the wind velocity is multiplied by a probability factor c_{prob} equal to 1.039, as indicated by the Eurocode 1. Afterwards, the reference kinetic pressure is calculated:

$$q_b \text{ (N/m}^2\text{)} = 1/2\rho v_b^2, \tag{17}$$

where ρ is the air density, conventionally equal to 1.25 kg/m³. It leads to $q_b = 421.69$ N/m². Finally, the wind pressure is given as the product between the term q_b and some coefficients regarding the exposition, shape and dynamic properties of the structure:

$$p = q_b c_e c_p c_d. \tag{18}$$

The aerodynamic coefficient c_p is equal to 0.8 for upwind surfaces and -0.5 for downwind and parallel-to-wind surfaces. The dynamic factor $c_s c_d$ is used in place of c_d and it is assumed conservatively equal to 1.1. The exposure coefficient c_e can be calculated as

$$c_e(z) = \begin{cases} k_r^2 c_0(z) \ln(z/z_0) [c_0(z) \ln(z/z_0) + 7] & \text{for } z \geq z_{min} \\ c_e(z_{min}) & \text{for } z < z_{min} \end{cases}, \tag{19}$$

in which k_r is 0.23, z_{min} 12 m, z_0 0.7 m and $c_0(z)$ is assumed equal to 1.

In Table 4 the corresponding resultant loads acting along the principal axes of the global coordinate system are summarised. In particular, it should be noted that the high values at the first floor are due to a loaded surface having an height of about 30 m.

The structural scheme takes into account the following stiffening typologies: shear walls, thin-walled open section shear walls and braced frames.

As regards shear walls having thin-walled closed or open sections, details on the procedure for the computation of the stiffness matrix can be found in Carpinteri et al. [32,33], in which Timoshenko–Vlasov’s theory [29,30] of sectorial areas is applied, according to the approach by Capurso [31].

Similarly, the frame structures are introduced by means of the approach by Pozzati [36], as previously suggested by Carpinteri and Carpinteri [28]. The author considers a frame equivalent to a shear wall, having the stiffness of each inter-floor segment equal

Table 4
Storey height and wind action for each floor.

Floor No.	Storey height (m)	Wind actions			Floor No.	Storey height (m)	Wind actions		
		F_x (kN)	F_y (kN)	M_z (kN m)			F_x (kN)	F_y (kN)	M_z (kN m)
39	6.75	299.60	513.50	9453.76	20	3.74	248.40	425.90	7842.64
38	5.03	297.50	510.00	9390.38	19	3.74	244.70	419.40	7721.30
37	5.10	295.40	506.40	9324.09	18	3.74	240.70	412.70	7599.60
36	5.10	293.20	502.70	9256.72	17	3.74	236.60	405.60	7468.11
35	5.53	291.00	498.90	9186.45	16	3.74	232.20	398.10	7330.47
34	3.89	288.70	495.00	9115.10	15	3.74	227.60	390.20	7184.86
33	3.74	286.40	491.00	9040.84	14	3.74	222.70	381.80	7030.20
32	3.74	284.00	486.80	8962.60	13	3.74	217.60	372.90	6864.66
31	3.74	281.50	482.60	8886.18	12	3.74	212.00	363.40	6690.80
30	3.74	279.00	478.30	8806.85	11	3.74	206.00	353.20	6503.90
29	3.74	276.40	473.80	8723.54	10	3.74	199.60	342.10	6298.16
28	3.74	273.70	469.20	8639.15	9	3.74	192.50	330.00	6076.13
27	3.74	270.90	464.40	8550.77	8	3.74	184.70	316.70	5832.00
26	3.74	268.00	459.50	8461.30	7	5.46	176.10	301.90	5558.89
25	3.74	265.10	454.40	8366.04	6	5.69	166.30	285.10	5249.56
24	3.74	262.00	449.10	8268.60	5	3.74	155.00	265.70	4892.05
23	3.74	258.80	443.60	8167.18	4	3.74	141.60	242.70	4468.26
22	3.74	255.50	438.00	8064.68	3	2.64	124.90	214.10	3941.97
21	3.74	252.00	432.00	7954.20	2	4.84	102.70	176.00	3240.00
					1	7.40	187.30	321.20	5915.31

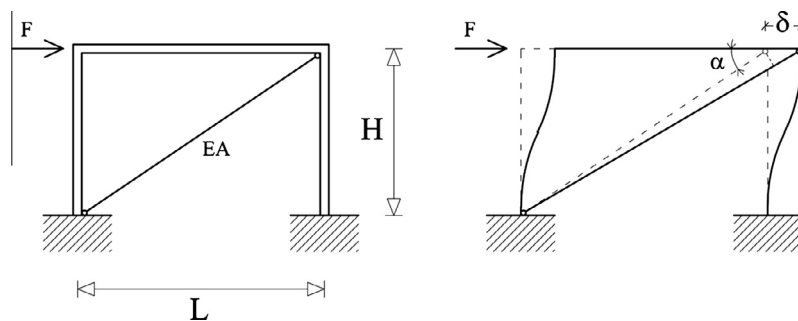


Fig. 7. Scheme of a braced frame with a single diagonal element.

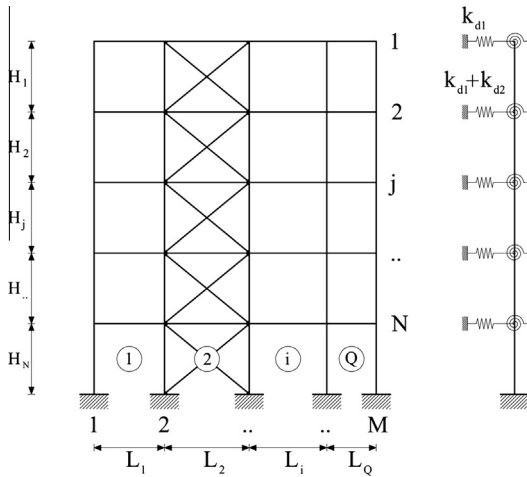


Fig. 8. Model of a braced frame equivalent to a shear wall.

to the sum of the stiffness of the columns of the corresponding floor and subjected to elastic rotational springs due to the rotational stiffness of the bays. Therefore, the stiffness matrix of the equivalent shear wall is obtained by adding the resistant contribution of the bays to the stiffness matrix related to the columns. More details on the procedure of constructing the condensed stiffness matrix of a frame are reported in Appendix A.

The aforementioned formulation has been extended in order to encompass braced frames. Let EA be the axial rigidity of the diagonal elements, we assume that only bracings in tension are engaged in the analysis. The simplified scheme of Fig. 7 shows the deformed configuration of a braced frame stiffened by a single diagonal element.

Due to the displacement δ of the frame, the diagonal bracing is subjected to an axial deformation, which is a function of the angle α . As a result of this, an axial force arises in the element:

$$N_d = \delta(EA/\sqrt{L^2 + H^2}) \cos \alpha. \tag{20}$$

The horizontal component of this force constitutes the resistant contribution of the diagonal bracing with regard to the lateral displacement of the frame:

$$F = \left[(EA/\sqrt{L^2 + H^2}) \cos \alpha^2 \right] \delta = k_d \delta. \tag{21}$$

Therefore, the structural scheme proposed by Pozzati may be modified, adding to each floor a fictitious horizontal spring whose stiffness is the sum of the terms k_d related to the diagonals connected to the floor (Fig. 8). This resistant contribution can be directly added to the coefficients of the main diagonal of the matrix k_{dd} described in Appendix A.

In the case of diagonals which refer to n non-consecutive floors, it is better to define a reduced $n \times n$ -stiffness matrix, which only represents the contribution of the bracings. The latter, adequately expanded to N -dimension, may be added to the $N \times N$ -stiffness matrix of the corresponding simple frame and, then, included in the general formulation of Section 1.

As regards the huge truss beams, the absence of detailed structural information has prevented the definition of an adequate model able to take into account their contribution to horizontal resistance.

Results of the analysis are summarised in the following pages. In Fig. 9(a–c) displacements in the X and Y directions and rotations at the floor levels are reported respectively. These curves are compared to those shown in the final project by the designers whose computation has been led by FE simulations. In particular, Studio

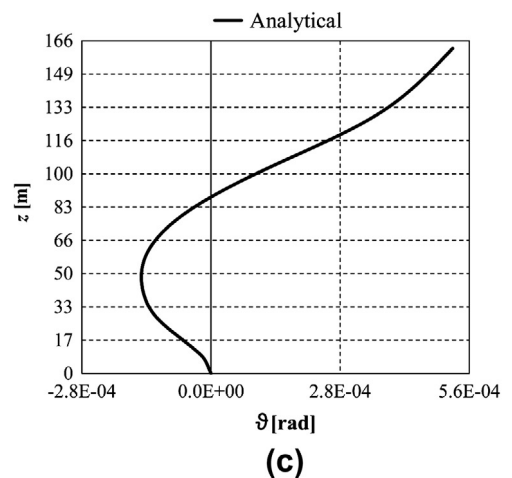
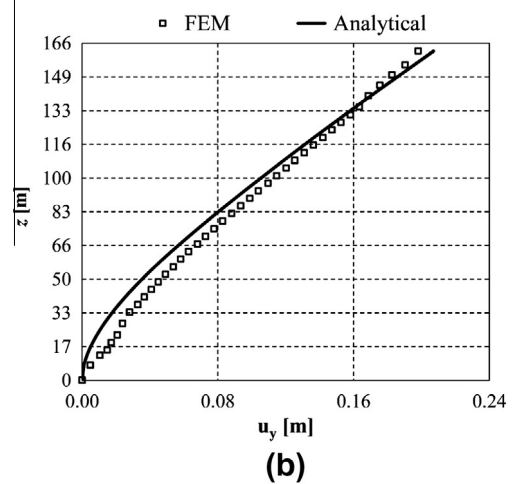
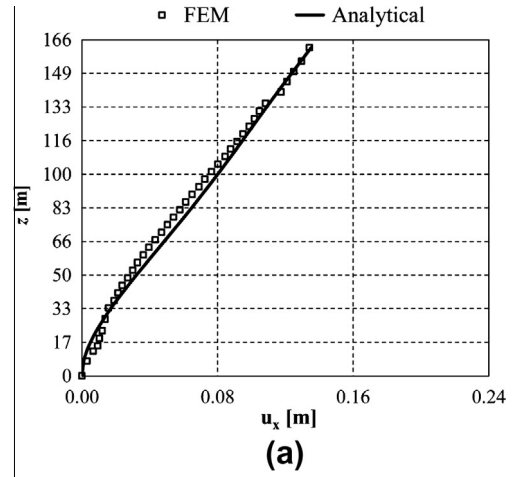


Fig. 9. Displacements of the floors in the global coordinate system. Translations in the X (a), Y (b) directions and rotation (c).

Ossola (Turin, Italy) in collaboration with Expedition Engineering (London, England) performed the structural project by means of Oasys-GSA program (Version 8.3). In the analysis, the stiffeners have been modelled as three-dimensional structures by means of 9000 beam- and 7000 shell-elements, totalling 10,000 degrees of freedom.

As can be seen, the analytical method achieves a satisfactory accuracy, the gap being in the range of not more than ± 0.015 m. Main differences arise next to the level of the huge truss beams.

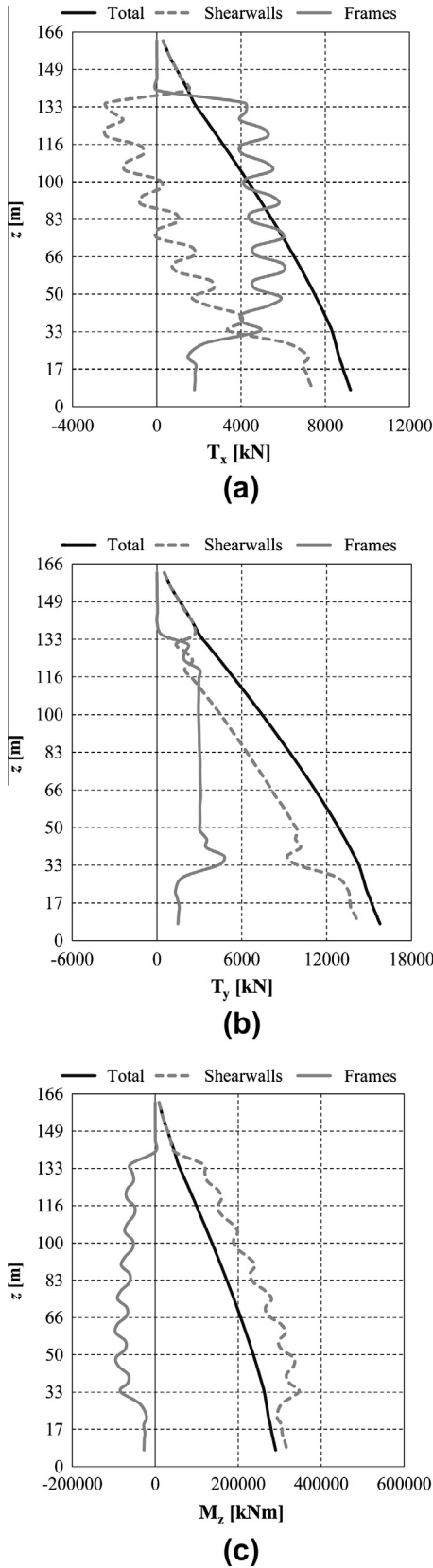


Fig. 10. Internal loading distribution between braced frames and shear walls: shear in the X (a), Y (b) directions and torsional moment (c).

In Fig. 10 the lateral load distribution of the internal actions between the main typologies of the structural scheme is presented. In particular, Fig. 10(a) and (b) report the distribution of the forces

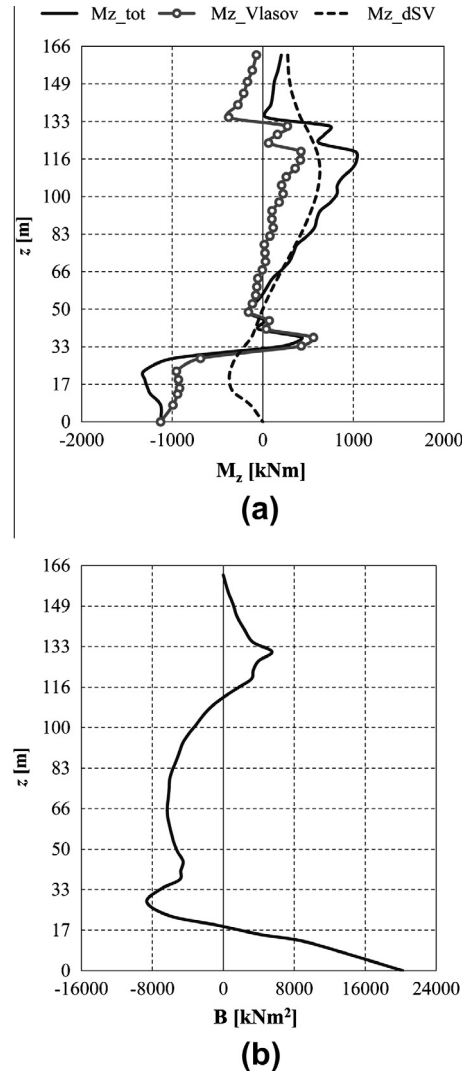


Fig. 11. Internal actions in thin-walled open section bracing No. 7: torsional moment (a) and bimoment (b).

along the principal directions, as well as Fig. 10(c) the distribution of the torque. Due to the structural discontinuity of the frames, in both principal directions high interaction forces arise between shear walls and frames. In the same manner, in X direction, further high interactions are caused by the presence of very rigid steel beams, as previously mentioned for frames 1 and 2. Such structural choices affect the torque distribution as well. The curves demonstrate the decisive contribution of the braced frames in the top part of the building, as well as, in the bottom part, the predominant resistance of the shear walls.

Looking at Figs. 11 and 12, it can be noted that the analytical formulation is also able to evaluate the main internal actions of a generic stiffener, such as shears, bending moments, torsional moments and, in the case of thin-walled open section elements, bimoments. In this way, it allows to assess which is, among all the stiffeners, the most affected by horizontal actions or the most suitable structural arrangement for the specific loading case. As regards the open section shear wall No. 7 (Fig. 4), in Fig. 11(a) the components of the internal torsional moment are highlighted: the first is related to pure torsion according to de Saint Venant theory, while the second is related to the non-uniform torsion, analysed in the framework of Timoshenko–Vlasov’s theory of the sectorial areas. As in the case of Fig. 10, it can be clearly seen the

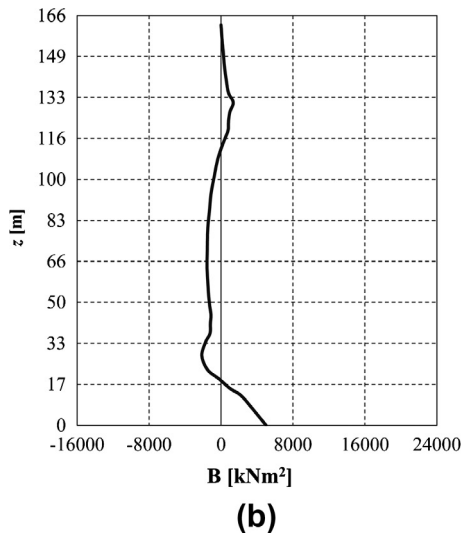
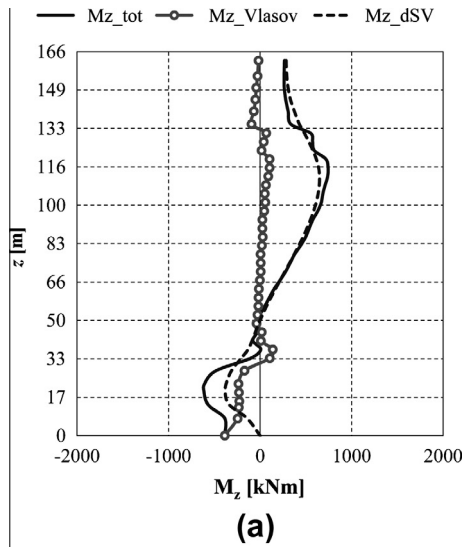


Fig. 12. Internal actions in thin-walled open section bracing No. 3: torsional moment (a) and bimoment (b).

discontinuities caused by the change in geometry and material of the frames, which in particular affects the non-uniform component. Furthermore, they also alter the evolution of the bimoment, as reported in Fig. 11(b). Lastly, in Figs. 12, the same curves related to the open section shear wall No. 3 show a more reduced contribution of the non-uniform component of the torsional moment, followed by a lower bimoment action. In other cases, such as shear walls No. 1, 8 and similar, pure torsion is sufficient to describe the torsional behaviour of the section as well as the bimoment may be completely neglected.

4. Conclusion

This paper focuses on the assessment of the global displacements and the lateral load distribution of external actions in high-rise buildings. To this purpose, the analytical formulation by Carpinteri et al. [32], which examines the structural behaviour of tall buildings sustained by any kind of bracings, is reviewed. In particular, it takes into consideration frames and thin-walled shear walls with closed or open section, the latter related to Timoshenko–Vlasov’s theory of sectorial areas and treated according to the approach by Capurso [31]. This work evaluates the accuracy

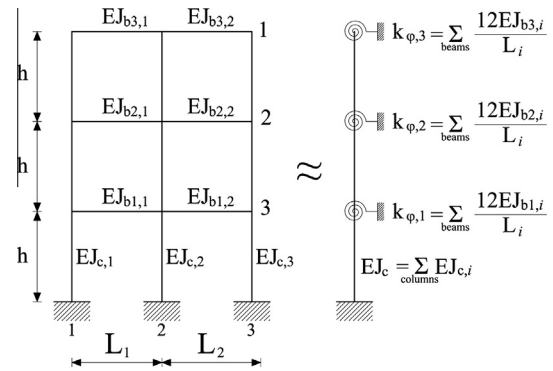


Fig. A1. Equivalence between a frame with rigid connections and a shear wall.

and the effectiveness of the aforementioned method through a numerical example regarding the Intesa Sanpaolo Tower, now under construction in Turin (Italy). For this specific case, the analytical model has been extended to encompass also braced frames. The results in terms of displacements have been compared to those obtained, in the final project, by means of FE simulations. The analytical formulation refers to three DOFs for each floor, totalling 117; on the contrary, the FE model takes into account about 10,000 DOFs. Despite of this, we achieved a good approximation. In addition, curves regarding the lateral load distribution between different structural typologies as well as the internal actions of a generic bracing have been reported in order to highlight the capabilities of the method.

Thus, the present paper confirms the usefulness of analytical models especially in the phases of evolution of the concept design in which the engineer attempts to gain insight into the key parameters governing the structural behaviour of complex buildings.

Acknowledgements

The financial support provided by the Ministry of University and Scientific Research (MIUR) for the PhD scholarship “Tall buildings constructed with advanced materials: a global approach for the analysis under static and dynamic loads” is gratefully acknowledged.

The authors are grateful to Intesa Sanpaolo Banking Group for having provided the scheme of the project and the preliminary structural calculations.

Special thanks go to Eng. Egon Paganone for his contribution to the production of the structural drawings and to the computational analysis.

Appendix A

The procedure of constructing the condensed stiffness matrix of an horizontal bracing is here explained, as proposed by Pozzati [36].

Let us consider a shear wall subjected to concentrated horizontal forces.

Each inter-floor segment is defined by the corresponding stiffness matrix \mathbf{k}_i , which refers to the horizontal displacements and rotations.

$$\mathbf{k}_i = \frac{EJ_i}{h^3} \begin{bmatrix} 12 & -12 & -6h & -6h \\ -12 & 12 & 6h & 6h \\ -6h & 6h & 4h^2 & 2h^2 \\ -6h & 6h & 2h^2 & 4h^2 \end{bmatrix}. \quad (\text{A.1})$$

The global stiffness matrix of shear wall can be obtained expanding and adding the contributions of all the segments. Therefore, in the

case of a 3-storey shear wall having constant geometric dimensions, the global stiffness matrix is:

$$\mathbf{K} = \frac{EJ}{h^3} \begin{bmatrix} 12 & -12 & 0 & -6h & -6h & 0 \\ -12 & 24 & -12 & 6h & 0 & -6h \\ 0 & -12 & 24 & 0 & 6h & 0 \\ -6h & 6h & 0 & 4h^2 & 2h^2 & 0 \\ -6h & 0 & 6h & 2h^2 & 8h^2 & 2h^2 \\ 0 & -6h & 0 & 0 & 2h^2 & 8h^2 \end{bmatrix}. \quad (\text{A.2})$$

The latter may be written highlighting some terms:

$$\mathbf{F} = \mathbf{K}\delta \rightarrow \begin{Bmatrix} \mathbf{F}_d \\ \mathbf{0} \end{Bmatrix} = \begin{bmatrix} \mathbf{k}_{dd} & \mathbf{k}_{dr} \\ \mathbf{k}_{rd} & \mathbf{k}_{rr} \end{bmatrix} \begin{Bmatrix} \delta_d \\ \delta_r \end{Bmatrix}, \quad (\text{A.3})$$

in which δ_d and δ_r stand for horizontal displacements and rotations respectively. From Eq. (A.3) the condensed stiffness matrix of the shear wall may be obtained and the relationship between actions and horizontal displacements is acquired:

$$\mathbf{K}^* = \mathbf{k}_{dd} - \mathbf{k}_{dr}\mathbf{k}_{rr}^{-1}\mathbf{k}_{rd}. \quad (\text{A.4})$$

$$\mathbf{F}_d = \mathbf{K}^*\delta_d = (\mathbf{k}_{dd} - \mathbf{k}_{dr}\mathbf{k}_{rr}^{-1}\mathbf{k}_{rd})\delta_d. \quad (\text{A.5})$$

In the case of a frame with rigid connections, the previous formulation can be used if we consider that the rotations of the nodes belonging to the same floor are equal each other. In this way, the rotational resistance due to each bay is equal to $6EJ_b/L$ for each node, being J_b and L the second moment of inertia and the length of the beam respectively. The contributions of all the bays can be added together and considered as the effect of a rotational spring applied to the corresponding floor. Therefore its effect can be directly included in the main diagonal of the sub-matrix \mathbf{k}_{rr} . On the other hand, excluding the bays, the frame can be easily treated as a shear wall in which the resistance of each segment is equal to the sum of the resistances of the corresponding columns.

In the case of a 3-storey frame with a constant floor height (Fig. A1), the corresponding global stiffness matrix may be defined by two components: the first one is related to the columns, whereas the second to the bays:

$$\mathbf{K} = \mathbf{K}_c + \mathbf{K}_b. \quad (\text{A.6})$$

The matrix \mathbf{K}_c may be written taking into account Eq. (A.2):

$$\mathbf{K}_c = \frac{(\sum EJ_{c,i})}{h^3} \begin{bmatrix} 12 & -12 & 0 & -6h & -6h & 0 \\ -12 & 24 & -12 & 6h & 0 & -6h \\ 0 & -12 & 24 & 0 & 6h & 0 \\ -6h & 6h & 0 & 4h^2 & 2h^2 & 0 \\ -6h & 0 & 6h & 2h^2 & 8h^2 & 2h^2 \\ 0 & -6h & 0 & 0 & 2h^2 & 8h^2 \end{bmatrix}. \quad (\text{A.7})$$

On the contrary, the matrix \mathbf{K}_b is a null matrix with the exception of the component \mathbf{k}_{rr} which is given by:

$$\mathbf{K}_b = \begin{bmatrix} \mathbf{0} & \mathbf{0} \\ \mathbf{0} & \mathbf{k}_{rr} \end{bmatrix} \rightarrow \mathbf{k}_{rr} = \begin{bmatrix} k_{\varphi,3} & 0 & 0 \\ 0 & k_{\varphi,2} & 0 \\ 0 & 0 & k_{\varphi,1} \end{bmatrix}. \quad (\text{A.8})$$

Therefore, by means of Eq. (A.4), the condensed stiffness matrix of the frame is computed.

References

- [1] Howson WP. Global analysis: back to future. *Struct Eng* 2006;84:18–21.
- [2] Khan FR, Sbarounis JA. Interaction of shear walls and frames. *J Struct Div ASCE* 1964;90:285–335.
- [3] Coull A, Irwin AW. Model investigation of shear wall structures. *J Struct Div ASCE* 1972;98:1233–7.
- [4] Heidebrecht AC, Stafford Smith B. Approximate analysis of tall wall-frame structures. *J Struct Div ASCE* 1973;99:199–221.
- [5] Rutenberg A, Heidebrecht AC. Approximate analysis of asymmetric wall-frame structures. *Build Sci* 1975;10:27–35.
- [6] Mortelmans FKEC, de Roeck GPJM, van Gemert DA. Approximate method for lateral load analysis of high-rise buildings. *J Struct Div ASCE* 1981;107:1589–610.
- [7] Rosman R. Approximate analysis of shear walls subjected to lateral loads. *ACI J* 1964;21:717–32.
- [8] Beck H, König G, Reeh H. Kenngrößen zur beurteilung der torsionssteifigkeit von hochhäusern. *Beton und Stahlbetonbau* 1968;63:268–77 (in German).
- [9] Beck H, Schäfer HG. Die berechnung von hochhäusern durch zusammenfassung aller aussteifenden bauteile zu einen balken. *Der Bauingenieur* 1969;44:80–7 (in German).
- [10] Stafford Smith B, Coull A. Tall building structures: analysis and design. New York: Wiley; 1991.
- [11] Hoenderkamp JCD, Snijder H. Approximate analysis of high-rise frames with flexible connections. *Struct Des Tall Build* 2000;9:233–48.
- [12] Lee J, Bang M, Kim JY. An analytical model for high-rise wall-frame structures with outriggers. *Struct Des Tall Spec Build* 2008;17(4):839–51.
- [13] Swaddiwudhipong S, Piriyaakontorn S, Lim Y, Lee S. Analysis of tall buildings considering the effect of axial deformation by the Galerkin method. *Comput Struct* 1989;32(6):1363–9.
- [14] Heidebrecht AC, Swift D. Analysis of asymmetrical coupled shear walls. *J Struct Div ASCE* 1971;97:1407–22.
- [15] Tso WK, Biswas JK. General analysis of non-planar coupled shear walls. *J Struct Div ASCE* 1973;99:365–80.
- [16] Capuani D, Savoia M, Laudiero F. Continuum model for analysis of multiply connected perforated cores. *J Eng Mech* 1994;120:1641–60.
- [17] Stamato MC, Mancini E. Three-dimensional interaction of walls and frames. *J Struct Eng ASCE* 1973;99:2375–90.
- [18] Gluck J, Krauss M. Stress analysis of group of interconnected thin-walled cantilevers. *J Struct Div ASCE* 1973;99:2143–65.
- [19] Khan FR. Tubular structures for tall buildings. *Handbook of concrete engineering*. New York: Van Nostrand Reinhold Co.; 1974.
- [20] Coull A, Bose B. Simplified analysis of framed-tube structures. *J Struct Div ASCE* 1977;101:2223–40.
- [21] Leung AYT. Microcomputer analysis of three-dimensional tall buildings. *Comput Struct* 1985;21:639–61.
- [22] Leung AYT, Wong SC. Local-global distribution factors method for tall building frames. *Comput Struct* 1988;29:497–502.
- [23] Wong CW, Lau SL. Simplified finite element analysis of three-dimensional tall building structures. *Comput Struct* 1989;33:821–30.
- [24] Pekau O, Zielinski ZA, Lin L. Displacements and frequencies of tall building structures by finite story method. *Comput Struct* 1995;54:1–13.
- [25] Pekau O, Lin L, Zielinski ZA. Static and dynamic analysis of tall tube-in-tube structures by finite story method. *Eng Struct* 1996;18:515–27.
- [26] Kim HS, Lee DG. Analysis of shear wall with openings using super elements. *Eng Struct* 2003;25:981–91.
- [27] Steenbergen RDJM, Blaauwendraad J. Closed-form super element method for tall buildings of irregular geometry. *Int J Solids Struct* 2007;44:5576–97.
- [28] Carpinteri A, Carpinteri An. Lateral load distribution between the elements of a three-dimensional civil structure. *Comput Struct* 1985;21:563–80.
- [29] Timoshenko S. *Theory of elastic stability*. 1st ed. New York: McGraw-Hill Book Company Inc.; 1936.
- [30] Vlasov V. *Thin-walled elastic beams*. 2nd ed. Washington: US Science Foundation; 1961 (Jerusalem: Israeli Program for scientific translation).
- [31] Capurso M. Sul calcolo dei sistemi spaziali di controventamento (parte 1). *Giornale del Genio Civile* 1981;1–2-3:27–42 [in Italian].
- [32] Carpinteri A, Lacidogna G, Puzzi S. A global approach for three-dimensional analysis of tall buildings. *Struct Des Tall Spec Build* 2010;19:518–36.
- [33] Carpinteri A, Corrado M, Lacidogna G, Cammarano S. Lateral load effects on tall shear wall structures of different height. *Struct Eng Mech* 2012;41:313–37.
- [34] Ministero delle Infrastrutture. DM 14/01/2008: nuove norme tecniche per le costruzioni. *Gazzetta ufficiale* 04.02.2008; No. 29 [in Italian].
- [35] European Committee for Standardization. Eurocode 1: actions on structures. General actions. Densities, self-weight, imposed loads for buildings. BS EN 1991-1-1. London: British Standard Institution; 2002.
- [36] Pozzati P. *Teoria e tecnica delle strutture*. Torino: Editrice Torinese; 1977 [in Italian].